Scheduled for the October 2004 issue of The Astronomical Journal
Preprint typeset using LaTeX style emulateapj v. 11/12/01

PHYSICAL STRUCTURE OF PLANETARY NEBULAE. II. NGC 7662

Martín A. Guerrero[1,2], Elizabeth G. Jaxon[2], and You-Hua Chu[2,3]
[1] Instituto de Astrofísica de Andalucía, CSIC, Granada 18008, Spain
[2] Astronomy Department, University of Illinois at Urbana-Champaign, Urbana, IL 61801
mar@iaa.es, ejaxon@uiuc.edu, chu@astro.uiuc.edu
Scheduled for the October 2004 issue of The Astronomical Journal

ABSTRACT

We present a study of the structure and kinematics of the triple-shell planetary nebula NGC 7662 based on long-slit echelle spectroscopic observations and *HST* archival narrow-band images. The structure of NGC 7662 main nebula consists of a central cavity surrounded by two concentric shells. The bright inner shell has a non-negligible thickness and the highest density in the nebula. The outer shell is filled with nebular material whose density profile shows a $\propto r^{-1}$ drop-off in the inner regions of the shell and flattens in the outermost regions. Both the inner and the outer shells can be described as prolate ellipsoids: the inner shell is more elongated, while the outermost layer of the outer shell expands faster. The physical structure of NGC 7662 is qualitatively consistent with the predictions of hydrodynamical simulations based on the interacting-stellar-wind models for planetary nebulae with a 0.605 $M_\odot$ central star. Models with a higher AGB wind velocity are needed for detailed comparisons.

Subject headings: ISM: planetary nebulae: general – ISM: planetary nebulae: individual (NGC 7662)

1. INTRODUCTION

Planetary nebulae (PNs) exhibit a wide variety of morphologies including round, elliptical, bipolar, and point-symmetric shapes (Balick 1987; Schwarz, Corradi, & Melnick 1992; Manchado et al. 1996). These main morphological classes can be accounted for by the interacting-stellar-winds model (Kwok, Purton, & Fitzgerald 1978) assuming that a pole-to-equator density gradient exists in the Asymptotic Giant Branch (AGB) wind (Balick 1987). The detailed morphology of some PNs has proven to be very complex and rich, however. By analyzing the morphology and kinematics of a PN, it is possible to establish its physical structure and gain insight into its evolutionary stage.

We have started a program to analyze high-resolution images and high-dispersion spectra of PNs in multiple nebular lines, in order to determine the physical structure of PNs. By comparing the results with hydrodynamical models, we hope to understand better the formation and evolution of PNs. The first PN we have studied is the Owl Nebula (Guerrero et al. 2003, hereafter Paper I). The second PN we have selected to study is NGC 7662, which is distinct from the Owl Nebula not only in morphology but also in excitation structure.

NGC 7662 has a bright main nebula that shows elliptical, double-shell morphology which is successfully reproduced by the interacting-stellar-winds model (e.g., Frank & Mellema 1994). The high surface brightness and moderately large size of this nebula, 30″ in diameter, make it ideal for a detailed case study of the physical structure of elliptical PNs. We have used narrow-band images and high-dispersion spectra of NGC 7662 to build a 3-D spatio-kinematic model, derived the density and ionization fraction profiles, and interpreted the results in the light of the interacting-stellar-winds model. This paper reports our study of NGC 7662.

2. OBSERVATIONS

The *Hubble Space Telescope* (*HST*) archive contains images of NGC 7662 obtained through narrow-band filters in the Hα, [O III] λ5007, He II λ4686, and [N II] λ6584 lines (Program ID #6117, PI: B. Balick; Program ID #6943, PI: S. Casertano; Program ID #8390, PI: A. Hajian). These filters have central wavelengths and FWHM bandwidths of 6565.6 Å and 29 Å (Hα), 5012.9 Å and 37 Å ([O III]), 4694.5 Å and 35 Å (He II), and 6590.9 Å and 40 Å ([N II]), respectively. We retrieved all archival *HST* images of NGC 7662 in these lines and combined them respectively to result in total exposure times of 200 s (Hα), 500 s ([O III]), 200 s (He II), and 2,800 s ([N II]). The [N II] image is seriously contaminated by the bright Hα flux transmitted at the blue wing of the [N II] filter because NGC 7662 is a high-excitation PN with [N II]/Hα as low as ∼0.007 in the shells and 0.116 in the [N II]-bright knots (Hyung & Aller 1997). We have thus used the transmission curve of the [N II] filter to estimate this Hα contribution and subtracted a scaled Hα image from the [N II] image to produce a net [N II] image. The Hα, [O III], He II, and the net [N II] images are presented in Figure 1.

High-dispersion spectroscopic observations of NGC 7662 were obtained with the echelle spectrograph on the 4-m telescope at the Kitt Peak National Observatory (KPNO) on 1986 October 21–23. The spectrograph was used in the single-order, long-slit mode, covering only the [O III] λ4959, 5007 lines. The 79 line mm^{-1} echelle grating and the long-focus red camera were used; the resultant reciprocal dispersion was 2.47 Å mm^{-1}. The spectra were recorded with the 800×800 TI #2 CCD with a 2×2 binning. The resulting pixel size of 30 μm corresponded to a spatial scale of 0.″33 pixel^{-1} and a sampling of 4.5 km s^{-1} pixel^{-1} along the dispersion direction. A slit width of 150

[3] Visiting Astronomer, Kitt Peak National Observatory, National Optical Astronomy Observatories, which is operated by the Association of Universities for Research in Astronomy, Inc. (AURA) under cooperative agreement with the National Science Foundation.

μm (1″) was used, and the resultant instrumental FWHM was 9.5±0.3 km s^{-1}. The angular resolution, determined by the seeing, was 1.″9.

We obtained four long-slit spectra of NGC 7662: one along the major axis (PA=44°), two parallel to but with a 3″ offset from the major axis, and one along the minor axis (PA=135°). The slit positions are marked on the [O III] image in Figure 1. The exposure times were 300 s for the spectrum along the major axis, and 200 s for the other three. The spectra were reduced using standard IRAF packages[2]. The curvature-corrected, wavelength-calibrated echellograms are displayed in Figure 2. The velocities are referenced to the systemic velocity of NGC 7662.

3. RESULTS

3.1. *Morphology*

NGC 7662 is a triple-shell nebula with a bright 17.″9×12.″4 inner shell enveloped by a 30.″8×27.″2 outer shell and surrounded by a faint spherical halo 134″ in diameter (Chu, Jacoby, & Arendt 1987). The major-to-minor axial ratio of the inner shell, ∼1.4, is noticeably larger than that of the outer shell, ∼1.1. The inner shell appears as a bright "rim"[3] with an apparent thickness of ∼2.″5, about half the length of the semi-minor axis. In contrast, the outer shell appears as an envelope attached to the inner shell, showing no limb-brightening.

The morphology of the main nebula is complicated by the presence of "fast low-ionization emission regions (FLIERs)," as discussed in detail by Balick et al. (1998). Our aim is to study the basic underlying structure of the nebula, therefore we select the sectors of the main nebula that are free of FLIERs. In particular, the analysis of the density and ionization structure of the nebula in Section §3.3 will be focused in its northwest quadrant.

3.2. *Kinematics*

The kinematics of NGC 7662 has been studied by Balick, Preston, & Icke (1987) using echelle spectra of the Hα and [N II] lines. As the Hα line has a large thermal width and the [N II] emission is dominated by the FLIERs, we have chosen to use [O III] to study the kinematics.

Our [O III] echellograms, displayed in Figure 2, show two kinematic systems corresponding to the inner and outer shells. The inner shell appears as a hollow position-velocity ellipse that has a marked tilt along the major axis (PA 45°), indicating that it is an expanding prolate ellipsoidal shell with its northeast side tilted towards us. The velocity dispersion within the shell is small; for example, the blue- and red-shifted components at the central position have an observed velocity FWHM of 13 km s^{-1}, corresponding to an intrinsic velocity FWHM of 8 km s^{-1} (after subtracting the instrumental and thermal widths). The brightness variations along the position-velocity ellipse can be naturally produced by the different line-of-sight path lengths through a prolate ellipsoidal shell (Frank & Mellema 1994).

The outer shell also appears as a position-velocity ellipse, with a hollow center and thick filled rims, but without an obvious tilt. This echelle line morphology is consistent with a thick expanding shell with a small ellipticity. For sightlines through the thick shell rims, the broad line profiles are caused by the wide range of projection angles between the radial expansion velocity and the line of sight. Near the shell center, the line profiles of the outer shell are superimposed on those of the bright inner shell; however, the narrow widths of the blue- and red-shifted components indicate that the outer shell expands at least as fast as the inner shell and that the velocity dispersion in the outer shell is small as well. The brightness variations within the thick shell rims in the echellograms can be caused by a combination of small density and velocity variations within the shell. The echellograms also show faint unresolved emission beyond the visible boundary of the outer shell. This extension originates from the faint halo of NGC 7662, and its FWHM ∼ 45 km s^{-1} is unusually large for faint PN halos (Chu & Jacoby 1989; Guerrero, Villaver, & Manchado 1998).

The observed position-velocity ellipse of an expanding shell can constrain its geometry and kinematics. Assuming a simple homologously expanding ellipsoidal shell (i.e., $v_{\rm exp} \propto r$), it is possible to derive the axial ratios, inclination angles and expansion velocities of the shell. For the inner shell of NGC 7662, the observed position-velocity ellipse is narrow and well defined, thus it can be directly compared with synthetic position-velocity ellipses to determine its geometry and kinematics. The outer shell is more difficult to model because its thick shell can be divided into multiple thin expanding shells, but the position-velocity ellipses of these thin shells cannot be resolved from one another. In the Owl Nebula, it has been shown that the outermost layer of its outer shell (most well defined in the low ionization [N II] line) is characterized by a position-velocity ellipse that encloses the echelle line image of that shell (Paper I). We have thus adopted such an ellipse as the position-velocity ellipse of the outermost layer of the outer shell of NGC 7662. Note that this assumption would be valid as long as there is no negative velocity gradient in the outer shell

Using these models, we have produced synthetic position-velocity ellipses to match these observed in the inner shell and the outermost layer of the outer shell. The position-velocity ellipses of the best-fit models are overplotted in Figure 2, and the relevant parameters are summarized in Table 1. For the inner shell, we find that its major axis is tilted by 50° against the line of sight along PA 45°, and that its expansion velocities are 35±3 km s^{-1} and 53±6 km s^{-1} in the equatorial plane and along the pole, respectively. For the outer shell, the small line tilt implies a small ellipticity or a pole-on geometry. To overcome this ambiguity, we assumed that the inclination of the symmetry axis of the outer shell is the same as that of the inner shell (Balick et al. 1998) and derived equatorial and polar expansion velocities for the outer shell of 50±5 km s^{-1} and 60±8 km s^{-1}, respectively. The outer shell of NGC 7662 has a smaller axial ratio than the inner shell, 1.2 versus 1.5. The outermost layer of the outer

[2] IRAF is distributed by the National Optical Astronomy Observatories, which is operated by the Association of Universities for Research in Astronomy, Inc. (AURA) under cooperative agreement with the National Science Foundation.

[3] The inner shell is called "rim" by Frank, Balick, & Riley (1990)

shell expands faster than the inner shell, which may be expected for dense gas diffusing into the surroundings with much lower density. The inner shell has a kinematic age of $\sim 700 \times \frac{d}{800}$ yr, where d is the distance in pc (d=800 pc, Hajian & Terzian 1996), and the outer shell has a kinematic age of $\sim 1{,}050 \times \frac{d}{800}$ yr.

3.3. *Density and Ionization Structure*

The spatio-kinematic models of NGC 7662 deduced in §3.2 can be used along with the observed surface brightness distribution in different emission lines to derive the density and ionization structure within this nebula. The northwest quadrant of NGC 7662 provides the most appropriate region for this analysis because it has no FLIERs and shows smooth, featureless emission in both the direct images and [O III] echellogram. Furthermore, this quadrant contains the minor axis along which the surface brightness distribution is less sensitive to the detailed shape and orientation of the nebular shells. The observed surface brightness profiles of the Hα, [O III], He II, and [N II] lines along this minor axis are displayed in Figure 3. Below is our analysis of the shell structure of NGC 7662 along the minor axis in the northwest quadrant.

To derive the density and ionization structure from the observed surface brightness, we have adopted a distance of 800 pc (Hajian & Terzian 1996), a logarithmic extinction $c(\mathrm{H}\beta)$=0.10, and an electron temperature of 12,500 K (Hyung & Aller 1997). We have approximated the main nebula of NGC 7662 by two ellipsoidal shells with the sizes, axial ratios and inclinations given in Table 1. We have further assumed that each shell consists of concentric subshells of constant density and ionization. As the surface brightness at a given radius r includes contributions from sub-shells of radii $\geq r$, the derivation of the density is best done from outside in.

The surface brightness profile of the Hα line is used to determine the radial profile of density $n(r)$. We adopt a power law for the density profile, i.e., $n(r) = n(r_0)r^{-i}$, where $n(r_0)$ and i will be determined from the fit to the surface brightness profile. The presence of multiple kinks in the Hα surface brightness profile implies that the density profile cannot be described by a single power law throughout the nebula. We have thus derived the density profile piecewisely. We experimented various power-law index i and find that $i = 0$ and 1 provide the best fits for the inner and outer shell, respectively. The best-fit density profile is shown in Figure 4. The corresponding surface brightness profile, overplotted in Figure 3, is in good agreement with the observed Hα profile from radii of $2''$ to $14''$.

It is interesting to note that the density profile in the outer shell is better described by a power law index of 1, instead of 2, as expected for an AGB wind with constant velocity and mass-loss rate. Three segments marked by small density jumps at radii $\sim 10\farcs8$ and $\sim 12\farcs2$ are present in the density profile of the outer shell. From the outer shell to the inner shell there is a sharp increase in density.

The inner shell is best described with a constant density $\sim$5,000 cm^{-3} over a thickness $\gtrsim 2''$, but the density drops off steeply at its inner edge. This shell density is within the range determined from spectrophotometric observations of the [S II] doublet, $\sim$4,000 cm^{-3} for the inner shell and >6,000 cm^{-3} in isolated dense regions (Lame & Pogge 1996; Hyung & Aller 1997). The density in the central cavity is low, but it cannot be determined with certainty because the surface brightness at the central region of the nebula is overwhelmed by the emission from the inner and outer shells. The sharp leading edge of the inner shell is in agreement with its supersonic expansion within the inner edge of the outer shell.

The density profile and the assumed ellipsoidal shell geometry can be used to determine the ionized mass in the inner and outer shells. The mass in the inner shell is $\sim$0.01 $M_\odot$, while that of the outer shell is $\sim$0.04 $M_\odot$. To test whether the inner shell consists entirely of swept-up AGB wind, we have extrapolated the density profile of the outer shell to the center and determined the swept-up mass. An excellent agreement exists between the expected swept-up mass and the mass in the inner shell, suggesting that no extraneous mass-loss is needed to form the inner shell.

The ionization structure of NGC 7662 can be studied using the observed surface brightness profiles of the He II, [O III], and [N II] lines (Fig. 3). The surface brightness, in conjunction with electron temperature and density, can be used to derive the ionic abundance. We have adopted appropriate electron temperatures for lines of different excitations: 14,000 K and 11,000 K for the high-excitation [O III] and He II lines in the inner and outer shells, respectively, and 8,500 K for the low-ionization [N II] line (Barker 1986; Hyung & Aller 1997). The ionic abundances determined using these temperatures and the above derived densities are then divided by the corresponding elemental abundances (Barker 1986) to compute the ionization fractions of He^{++}, O^{++}, and N^{+} shown in Figure 4.

An inspection of Fig. 4 shows that the ionization fraction of He^{++} is rather constant and greater than 0.8 through the nebula, while those of O^{++} and N^{+} increase outwards, as expected from stratified ionization. It must be noted that the detailed level and shape of the ionization fraction profiles depends on the choice of elemental abundances and electron temperatures. The large ionization fraction of He^{++}, for instance, may imply full ionization of He, as typically predicted by ionization models (e.g., Alexander & Balick 1997), with He abundances smaller by $\sim$10% than those here adopted. Similarly, variations of the electron temperature with radius in NGC 7662, as reported by Barker (1986), may affect the derived ionization fraction profiles, especially those of O^{++} and N^{+}, so that larger values of electron temperature mimic larger ionization fractions of O^{++} and N^{+}. The increased ionization fraction of O^{++} in the outermost regions of NGC 7662 seems real, however, as the electron temperature is known to decrease outwards (Barker 1986). Therefore, the sharp increase of the ionization fraction of O^{++} at $r \sim 7''$ signifies the transition of ionization stage at the edge of the O^{+3} Strömgren sphere, although the exact shape of the O^{++} ionization fraction profile and the radius of the O^{+3} Strömgren sphere might be questionable.

4. DISCUSSION

Hydrodynamical simulations of the physical structure of PNs have been carried out in the framework of interacting stellar winds taking into account the evolution and mass-loss history of the central star (e.g., Frank et al. 1990;

Mellema 1994; Villaver, Manchado, & García-Segura 2002; Perinotto et al. 2004). In these simulations, the fast stellar wind excavates a central cavity and snowplows the AGB wind to produce a double-shell nebula. The inner shell, being the swept-up AGB wind, is denser than the outer shell. The outer shell has a relatively flat density profile as its sudden ionization has resulted in strong pressure gradients that have modified the original r^{-2} law. This overall structure is observed in NGC 7662; the Hα image and echelle spectra are similar to those simulated by Mellema (1994), and the mass in the inner shell is in agreement with the expected swept-up mass of the AGB wind.

We attempt to quantitatively compare the density profile and kinematic structure of NGC 7662 to PN models. The density profile of NGC 7662 is characterized by:

- a density contrast of $\sim$2 between the outer and inner shells,
- an inner shell with a thickness of 0.012 pc, about 0.3–0.5 times the shell radius, and
- an almost flat density profile in the outer shell, significantly flatter than the r^{-2} law.

The radial profile of the expansion velocity of NGC 7662 cannot be determined observationally because of the limited spatial resolution of the echelle observations and the non-negligible thermal line widths. Our analysis in §3.2 provides only the following basic kinematic characteristics of NGC 7662:

- the inner shell has a small internal velocity dispersion, and expands at 35 km s^{-1} and 53 km s^{-1} along the equator and poles, respectively; and
- the outer shell also has small internal velocity dispersions, and expands at similar velocities to the inner shell, but its outermost layer expands faster, at 50 km s^{-1} and 60 km s^{-1} along the equator and poles, respectively.

We have compared the density profile and kinematic structure of NGC 7662 to those synthesized from the Perinotto et al. (2004) models of spherical PNs that take into account different initial conditions and central star masses. They have divided the PN evolution into four phases: Phase I corresponds to the youngest stage when the central star is still too cool to ionize the AGB wind; Phase II corresponds to the compression stage when an ionized double-shell structure is visible; Phase III is the stage when the central star reaches the maximum temperature and the inner-to-outer shell density contrast is the highest; and in Phase IV recombination starts and a single shell is observed possibly with a recombination halo. The extended outer shell, high densities, density profile, and velocity structure of NGC 7662 are compatible with those of a PN at Phase II evolving toward Phase III (compare to Fig. 7 of Perinotto et al.).

Perinotto et al. (2004) modeled PNs for different central-star masses and presented their results in Figures 13–16. We can rule out a central star mass much below 0.6 M$_\odot$ because the densities in NGC 7662, a few 10^3 cm^{-3}, are more than an order of magnitude higher than those expected from PNs with low-mass central stars. We can also rule out a central star mass as high as 0.8–0.9 M$_\odot$, because such PNs have higher shell densities and shorter double-shell lifetime than NGC 7662. The observed properties of NGC 7662 are most compatible with the model for a 0.605 M$_\odot$ central star.

We can also compare NGC 7662 to the Perinotto et al. (2004) models for a 0.605 M$_\odot$ central star with different AGB mass loss rates (their Fig. 10). The density and velocity profiles of NGC 7662 are most compatible with the model with an AGB mass loss rate of 3×10^{-5} M$_\odot$ yr-1 and wind velocity of 10 km s^{-1}; however, the expansion velocities of NGC 7662 are much higher than the $\sim$15 km s^{-1} expansion velocities from this model. A higher shell expansion velocity can be achieved if the AGB wind velocity is higher, and to maintain the same AGB wind density profile a proportionally higher AGB mass loss rate is required. It is possible that the AGB wind velocity of NGC 7662 was 30–50 km s^{-1}, and the AGB mass loss rate was $\sim 10^{-4}$ M$_\odot$ yr^{-1}. Future models of NGC 7662 ought to consider these AGB wind properties.

5. SUMMARY

NGC 7662 is a triple-shell PN with a bright inner shell (or rim) surrounded by an outer shell and a faint, large halo. We have analyzed high-resolution images and spectra of the inner and outer shells of NGC 7662, and constructed 3-D spatio-kinematic models for its inner shell and the outermost layer of the outer shell. Both can be modeled as expanding prolate ellipsoidal shells with the northeast end of the major axis tilted toward us.

We have further used the spatio-kinematic models and the Hα, He II, [O III], and [N II] surface brightness profiles to determine the density profile and ionization structure along the minor axis. The density and kinematic structure of NGC 7662 are compared to Perinotto et al. (2004) models of spherical PNs. We find that NGC 7662 is in their Phase II evolutionary stage (the compression stage), as its outer shell is still fairly extended, but may be close to Phase III evolutionary stage as its inner shell does not seem to be compressed strongly from its interior. NGC 7662 is most compatible with models for a central star mass of 0.605 M$_\odot$. Future models with higher AGB wind velocities, such as 30–50 km s^{-1}, are needed for detailed comparisons with NGC 7662.

M.A.G. acknowledges support from the grant AYA 2002-00376 of the Spanish MCyT (cofunded by FEDER funds). Some of the data presented in this paper were obtained from the Multimission Archive at the Space Telescope Science Institute (MAST). STScI is operated by the Association of Universities for Research in Astronomy, Inc., under NASA contract NAS5-26555.

REFERENCES

Alexander, J., & Balick, B. 1987, AJ, 114, 713
Balick, B. 1987, AJ, 94, 671
Balick, B., Preston, H. L., & Icke, V. 1987, AJ, 94, 1641
Balick, B., Alexander, J., Hajian, A. R., Terzian, Y., Perinotto, M., & Patriarchi, P. 1998, AJ, 116, 360
Barker, T. 1986, ApJ, 308, 314

Chu, Y.-H., & Jacoby, G. H. 1989, IAU Symp. 131: Planetary Nebulae, 131, 198
Chu, Y.-H., Jacoby, G. H., Arendt, R. 1987, ApJS, 64, 529

Frank, A., Balick, B., & Riley, J. 1990, AJ, 100, 1903
Frank, A., & Mellema, G. 1994, ApJ, 430, 800
Guerrero, M. A., Chu, Y.-H., Manchado, A., & Kwitter, K. B. 2003, AJ, 125, 3213
Guerrero, M. A., Villaver, E., & Manchado, A. 1998, ApJ, 507, 889
Hajian, A. R., & Terzian, Y. 1996, PASP, 108, 258
Hyung, S., & Aller, L. H. 1997, ApJ, 491, 242
Kwok, S., Purton, C. R., & Fitzgerald, P. M. 1978, ApJ, 219, L125
Lame, N. J., & Pogge, R. W. 1996, AJ, 111, 2320
Manchado, A., Guerrero, M. A., Stanghellini, L., & Serra-Ricart, M. 1996, The IAC Catalog of Northern Galactic Planetary Nebulae, IAC Publishing, La Laguna, Tenerife
Mellema, G. 1994, A&A, 290, 915
Perinotto, M., Schönberner, D., Steffen, M., & Calonaci, C. 2004, A&A, 414, 993
Schwarz, H. E., Corradi, R. L. M., & Melnick, J. 1992, A&AS, 96, 23
Villaver, E., Manchado, A., & García-Segura, G. 2002, ApJ, 581, 1204

TABLE 1
SPATIO-KINEMATIC MODEL OF THE INNER AND OUTER SHELLS OF NGC 7662

	$V_{\rm equatorial}$ [km s^{-1}]	$V_{\rm polar}$ [km s^{-1}]	Inclination†	Angular Size	Linear Size‡ [pc]	Kinematic Age‡ [yr]
Inner Shell	35	53	50°	$13''\times19\farcs7$	0.050×0.076	700
Outer Shell	50	60	50°	$28''\times33\farcs6$	0.109×0.130	1,050

†Angle between the major axis and the line of sight.

‡Adopting a distance to NGC 7662 of 800 pc.

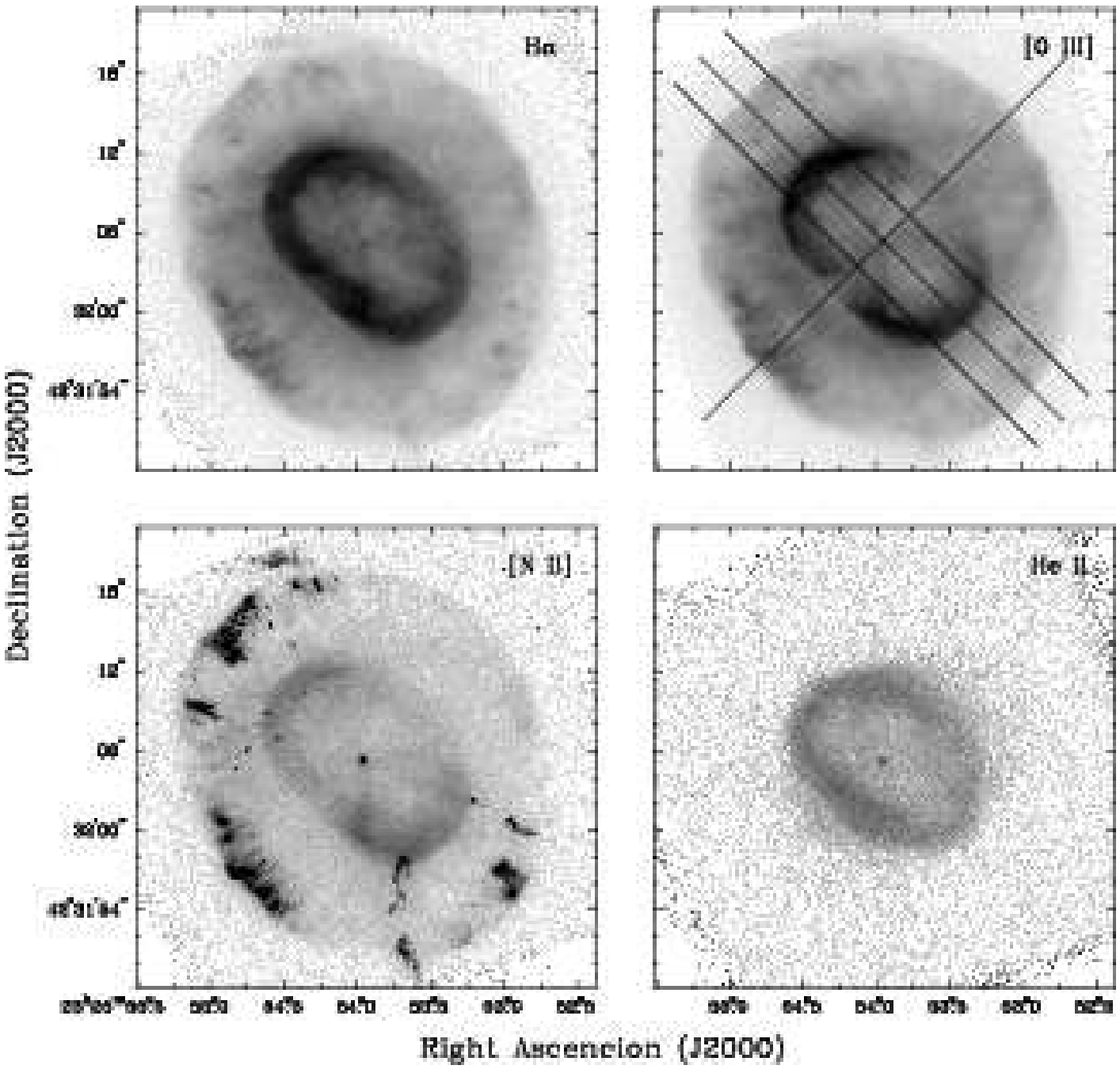

FIG. 1.— Negative grey-scale representation of the *HST* WFPC2 narrow-band images of NGC 7662. The contribution of the Hα line in the [N II] λ6584 filter has been subtracted. The slit positions of the echelle observations are marked on the [O III] image. The image displays are square root.

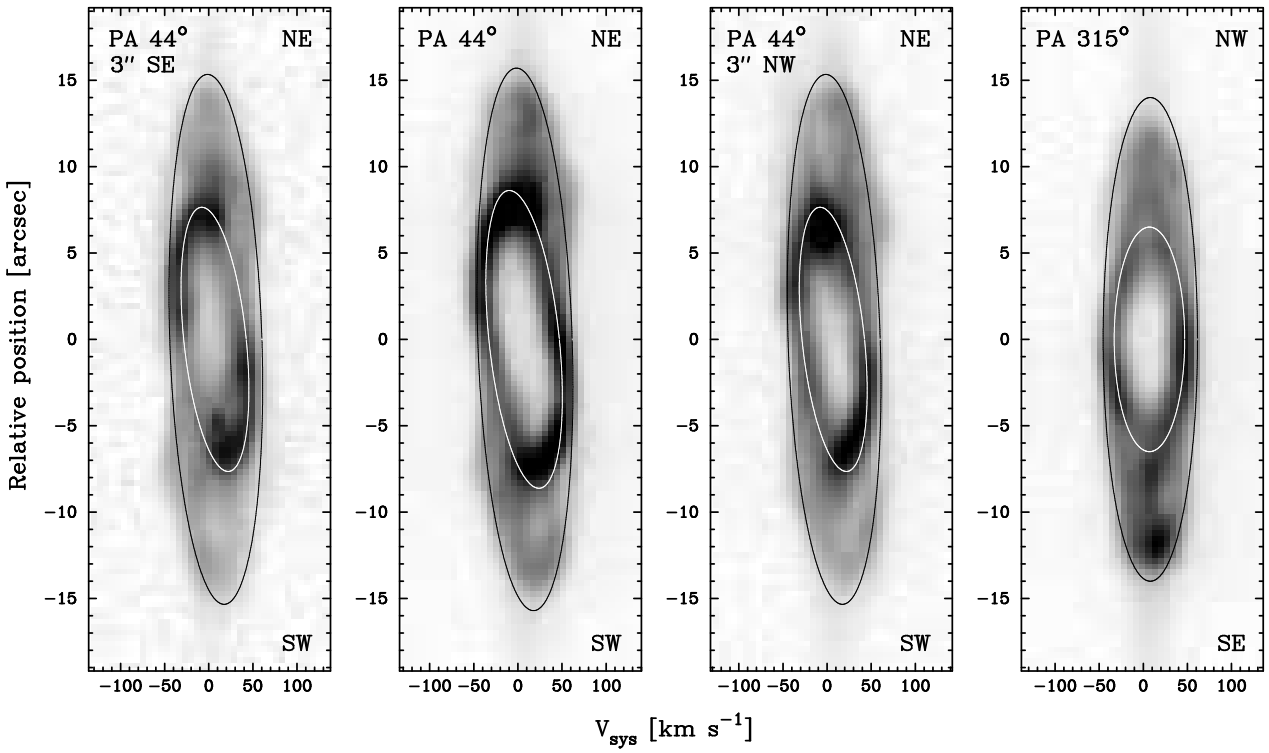

FIG. 2.— Negative grey-scale representation of the [O III] λ5007 emission line echellograms at PAs 44° and 315°. The ellipses overlaid on the echellograms correspond to the best-fit models for the inner and outer shells described in §3.2 (displayed in white and black, respectively).

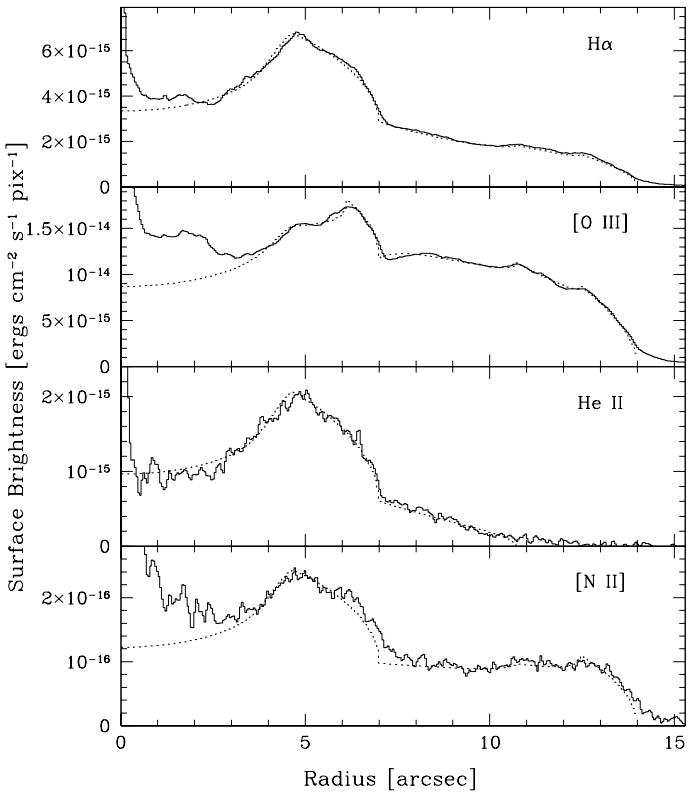

FIG. 3.— Surface brightness profiles along PA 315° of the Hα, [O III] λ5007, He II λ4686, and [N II] λ6584 lines (solid curves) extracted from the *HST* narrow-band images of NGC 7662. The dotted curves are our synthetic surface brightness profiles of these lines.

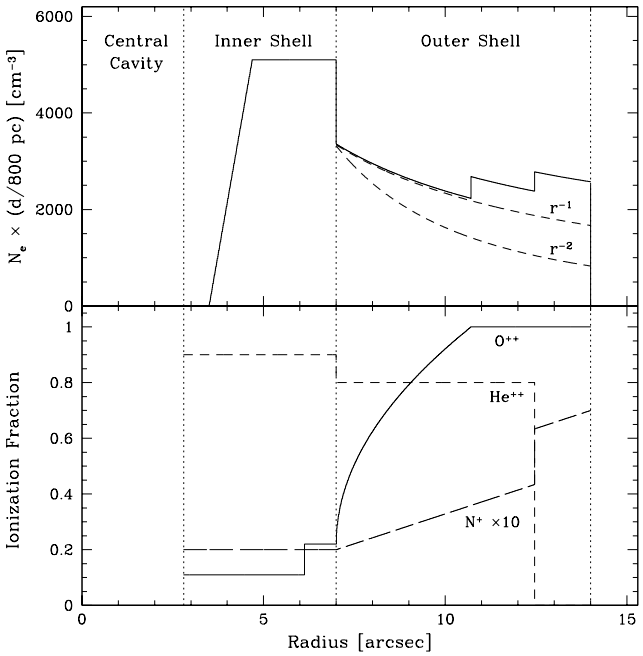

FIG. 4.— Radial profiles of the best-fit density and O^{++}, He^{++} and N^{+} ionization fractions of NGC 7662 along PA 315°. The positions of the central cavity, inner shell and outer shell are marked by vertical dotted lines. The dashed lines in the plot of the density profile correspond to a density dependence $\propto r^{-1}$ and $\propto r^{-2}$ for the outer shell. In the plot of the ionization fraction profiles, the N^{+} ionization fraction has been multiplied by 10 and plotted in long dashes. The O^{++} and He^{++} ionization fractions are plotted in solid and short-dahsed curves, respectively.